ECS Sensors Plus

OPEN ACCESS

Detection of Human Immunodeficiency Virus in Saliva Using a Nickel-Based Electrocatalyst

To cite this article: Dipu Saha *et al* 2024 *ECS Sens. Plus* **3** 040602

View the article online for updates and enhancements.

You may also like

- Different Sensing Technologies for Water Quality Monitoring: A Review
A. M. Faramawy, Nada M. Ali, Amany Khalifa et al.

- Editors' Choice—Challenges and Opportunities for Developing Electrochemical Biosensors with Commercialization Potential in the Point-of-Care Diagnostics Market
Amir Ali Akhlaghi, Harmanjit Kaur, Bal Ram Adhikari et al.

- Recent Developments in Sensor Technologies for Enabling the Hydrogen Economy
Kannan Ramaiyan, Lok-kun Tsui, Eric L. Brosha et al.

This content was downloaded from IP address 65.109.116.201 on 28/09/2025 at 01:50

ECS Sensors Plus, 2024 **3** 040602

Detection of Human Immunodeficiency Virus in Saliva Using a Nickel-Based Electrocatalyst

Dipu Saha,* Ashwin Ramanujam, and Gerardine G. Botte***,z**

Chemical and Electrochemical Technology and Innovation Laboratory (CETI-Lab), Institute for Sustainability and Circular Economy (ISCE), Department of Chemical Engineering, Texas Tech University, Lubbock, Texas 79409, United States of America

Acquired immunodeficiency syndrome (AIDS) is an ongoing and chronic condition caused by the human immunodeficiency virus (HIV). Early detection is one way to minimize the spread of AIDS. Current methods cannot reliably detect HIV in saliva samples due to the low concentration of viral particles in oral fluid. A simple, label-free, rapid response and unprecedented nickel-based electrochemical biosensor was developed to detect HIV in saliva using a NiOOH electrocatalyst. The current response difference at an applied potential vs a reference electrode in the presence of HIV was the trait of this sensor. It is hypothesized that the HIV p24 protein blocks the active surface area of the sensor, causing the current response to drop, which increases as the concentration of HIV increases in saliva. Comparative analyses using proteins with varying chemical moieties demonstrated that the sensor's response was triggered by the functional group's presence in the HIV p24 protein. The sensor's limit of detection in saliva is $\sim 48.40 \times 10^{-5}$ $TCID_{50}$ ml^{-1} HIV culture fluid. The sensor was utilized to successfully distinguish the current response of HIV in saliva from twelve different pathogens. Finally, the sensor replicated similar attributes with HIV-positive patient's saliva during a clinical study, which makes it a *state-of-the-art* non-invasive rapid response HIV sensor.

© 2024 The Author(s). Published on behalf of The Electrochemical Society by IOP Publishing Limited.. This is an open access article distributed under the terms of the Creative Commons Attribution 4.0 License (CC BY, https://creativecommons.org/licenses/by/4.0/), which permits unrestricted reuse of the work in any medium, provided the original work is properly cited. [DOI: 10.1149/2754-2726/ad9f80]

Manuscript submitted September 3, 2024; revised manuscript received December 11, 2024. Published December 27, 2024.

Supplementary material for this article is available online

Till 2023, more than 39 million people are living with human immunodeficiency virus (HIV), and the number of HIV-infected people is still increasing.[1] Approximately one in seven HIV-infected individuals do not know their HIV status, and such carriers have a higher chance of spreading HIV without knowing its consequences.[1,2] These HIV-infected individuals can develop AIDS faster as they are unaware of their status. To meet the 95-95-95 target of the Joint United Nations Programme on HIV/AIDS (UNAIDS) by 2025 and to minimize newer infections, facile and rapid response testing methods will be required to identify all HIV-infected people after their infection at the earliest.[3]

Traditionally, a blood test to detect HIV antibodies has been the gold standard confirmatory diagnostic method.[4] However, increased operational costs, turnaround time for results, delayed antibody response, and invasive sampling have called for quicker and more reliable screening diagnostic tests combined with confirmatory tests.[5] Screening tests are the first indicator that a person could potentially be infected by HIV.[6] The infection spread can be curbed if the infection has been detected at the earliest and necessary care can be provided. For this reason, screening tests have gained popularity over the years as early checks.[7,8] Nevertheless, these tests are still widely antibody-based and require the infection to progress before antibodies can be reliably detected.[9]

Hence, the focus shifted towards the detection of antigens in addition to antibodies to improve the detection of early infection.[5,10] The HIV antigens are generated within 2 to 3 weeks of exposure, even before antibodies are produced by the body.[11] During the performance of the modified Alere Determine™ HIV-1/2 Ag/Ab Combo rapid test in detecting acute/early HIV infections, the combo rapid test can detect HIV-1 infection earlier than other rapid tests with reactivity 15.5 days before Western blot positivity.[12] Although the device proved to detect acute/early HIV infections earlier than other rapid tests, this study did not estimate the sensitivity and specificity of the device in a prospective or cross-sectional study.[12] FDA-approved nucleic acid amplification testing (NAAT) is also available to detect HIV in serum or plasma during early detection.[13] However, these tests are expensive and require technical personnel to perform the test.[5] Additionally, blood or plasma is the sample source for these techniques, which makes sample collection difficult and increases contamination risks.

Oral fluid tests have been growing since OraQuick became approved to detect HIV antibodies by the U.S. Food and Drug Administration (FDA) for at-home use due to the ease-of-use, the non-invasive and non-infectious nature of these fluids compared to blood samples.[6,13–16] Although OraQuick is an antibody test that detects the infection only if tested after three months of exposure when antibodies have been generated, it provides evidence of using oral fluids to detect HIV. To the best of the authors' knowledge, there are no saliva-based HIV antigen detection methods available in the literature. It has been reported that if patients have not started any treatment and are newly infected, there is a high HIV viral load ((28,840–123,026) copies ml^{-1}) in their saliva.[17] Typically, HIV viral load is higher in the patient's bodily fluids during early infection.[18] One study found that over 70% of untreated individuals had detectable HIV ribonucleic acid (RNA) levels in saliva as compared to only 64% overall.[19] Few other studies also confirmed the presence of HIV RNA in saliva.[20–22] The possibility of HIV detection in saliva combined with the advantages of saliva over blood or serum sampling opens opportunities for a high-performing saliva-based HIV sensor in the market.

Electrochemical sensors for pathogen detection have been in the limelight for their advantage of being simple, cost-effective with low detection limits, and using low sample volumes.[23–25] They can detect different bacteria and viruses in blood and saliva, including SARS-CoV-2, Hepatitis virus, Zika virus, *E.coli*, and S. typhimurium.[25–29] More specifically, a few electrochemical sensors have been aimed at targeting HIV.[30,31] Zhang et al. developed a magnetic electrochemical biosensor, where an electrically controllable magnetic gold electrode (ECM-GE) was utilized to detect single nucleotide polymorphisms (SNPs) in HIV-related salivary deoxyribonucleic acid (DNA).[30] The ECM-GE allows for high sensitivity and specificity for single-base mismatches and can detect target HIV-related salivary DNA at concentrations as low as 0.37 fM with high reproducibility.[30] A multi-walled carbon nanotubes (MWCNTs) sensor was developed to detect HIV p24 antigen

*Electrochemical Society Student Member.
**Electrochemical Society Member.
***Electrochemical Society Fellow.
zE-mail: gerri.botte@ttu.edu

utilizing molecularly imprinted polymers (MIP) in human serum samples.[31] The limit of detection (0.083 pg ml^{-1}) of this sensor was significantly lower than other available techniques.[31] Although MIP-based sensors exhibit good detection selectivity and stability, their intricate electrodes are tedious to prepare and typically suffer from slow kinetics arising from resistances during the transport of analyte to the imprinted cavities of the electrode.[30,32] Facile electrode configurations would enable ease of electrode preparation and scale-up. Nickel-based electrocatalysts showed excellent redox behavior and are highly stable in alkaline conditions, which enhanced the sensor's reusability.[33,34] Nickel-based catalysts are also more affordable and plentiful than noble materials, making the sensor eligible for commercial applications.[33,34]

To overcome the challenges associated with different screening tests, a simple, non-invasive, rapid, nickel-based HIV diagnostic sensor has been developed. This electrochemical biosensor detects HIV in saliva using NiOOH electrocatalyst in an alkaline buffer media, combined with chronoamperometry and electrochemical impedance spectroscopy (EIS) techniques (Fig. 1). The biosensor exhibited a low detection limit of $\sim 48.40 \times 10^{-5}$ $TCID_{50}$ ml^{-1} HIV concentration in saliva, which lies in the ranges of HIV RNA in saliva reported in the literature.[17,19–21] The sensor showed a distinguishable response of HIV in saliva from twelve different pathogens without showing any cross-reactivity. Finally, the sensor detected HIV in HIV-positive patients' saliva during the clinical study.

Materials and Methods

Reagents.—Potassium hydroxide (KOH) NF/FCC pellets were purchased from Fisher Scientific (Fair Lawn, NJ, USA, CAS# 1310-58-3, Lot# 149366, contains 10%–15% water), ultrapure DI water from ELGA PURELAB Ultra (18.2 MΩ.cm) was used for the preparation of 1 M and 0.01 M KOH. Kimtech Science™ Kimwipes™ Delicate Task Wipes were purchased from Kimberly-Clark Professional (Roswell, GA, USA) to dry electrodes during the solutions change between the experiments. Sodium chloride (NaCl), certified ACS (CAS# 7647-14-5, Lot# 231772, contains 99% minimum), and 1 M Tris pH 7.0 (Catalog# AM9850G, Lot# 3055743) was purchased from Fisher Scientific (Fair Lawn, NJ, USA). Influenza A H1N1 (A/California/07/2009) Nucleoprotein / NP Protein (His Tag) (Catalog# 40205-V08B, Lot# LC16MY2623) and Hepatitis B Virus (HBV)(ayw/France/Tiollais/1979) Capsid protein (His Tag) (Catalog# 40573-V08E, Lot# LC16DE2601) was purchased from Sino Biological, Inc. (Chesterbrook, PA, USA). Purified recombinant protein of HIV-1 p24 protein, with C-terminal His tag, expressed in *E.coli*, was acquired from Origene Technologies Inc. (Rockville, MD, USA, Catalog# TP790122, Lot# WX02723E). The buffer solution of HIV-1 p24 protein (PBS, 1 mM DTT, pH 7.4, 10% glycerol) was provided by Origene Technologies Inc. (Rockville, MD, USA) to investigate the interferences of the buffer. A list of the pathogens studied is provided in Table S1 of **Supplementary Information** (**SI**).

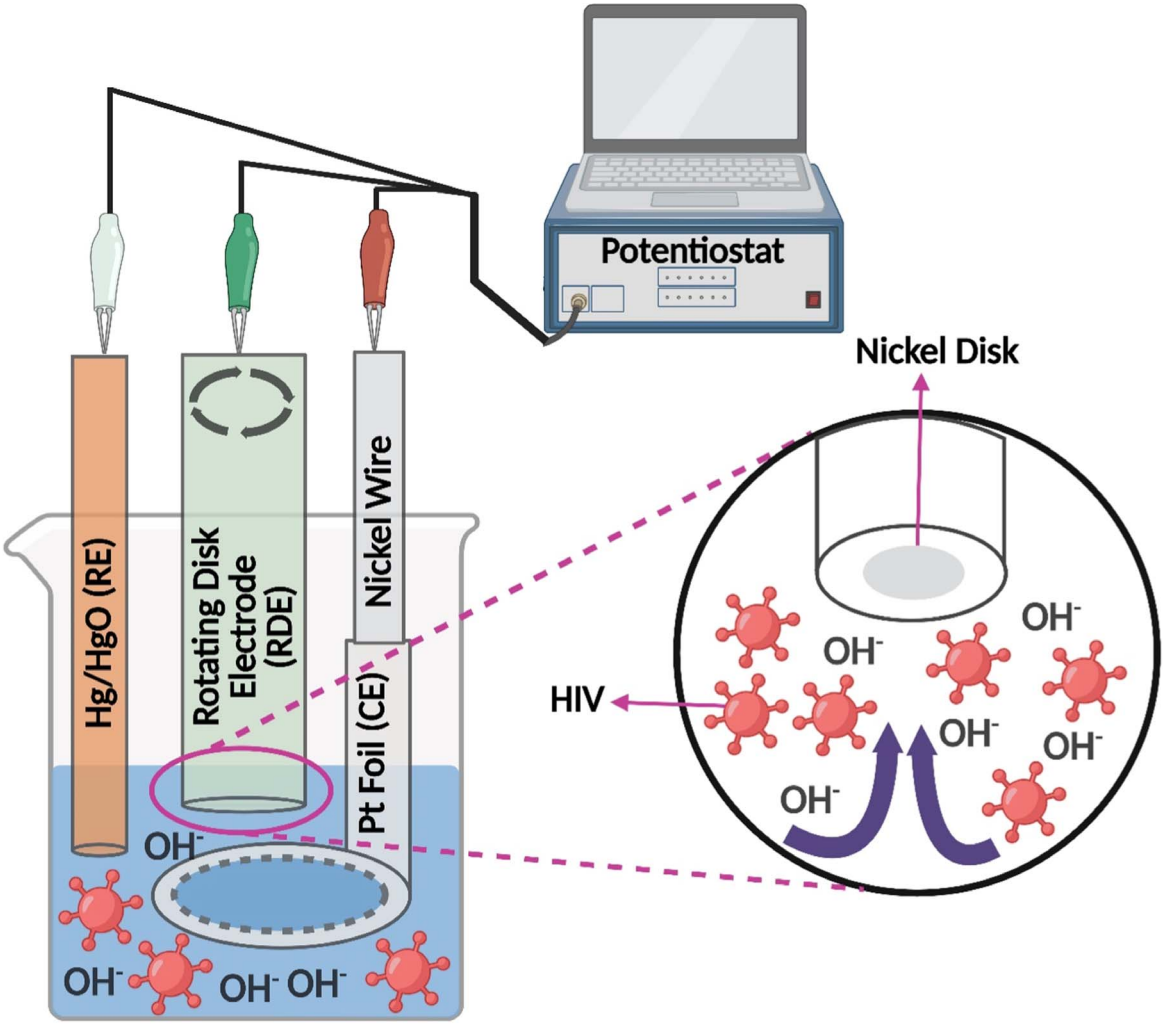

Figure 1. Illustration of the sensor during HIV Culture Fluid (HIV CF) detection. Schematic of a three-electrode setup submerged in an HIV CF and 0.01 M KOH solution, connected to a potentiostat. The zoomed view represents the attraction of OH^- ions and HIV CF to the nickel electrode at the applied potential during the rotation of the electrode.[35].

Pathogens such as Human Immunodeficiency Virus Type 1 Culture Fluid (HIV), NATtrol™ Hepatitis B Virus (HBV), Epstein Barr Virus Culture Fluid (EBV), Cytomegalovirus Culture Fluid (CMV), Herpes Simplex Virus Type 1 Culture Fluid (HSV-1), Influenza A H1N1pdm Virus Culture Fluid (INF-A), Influenza B Virus Culture Fluid (INF-B), Human Metapneumovirus 16 Type A1 Culture Fluid (hMPV), Respiratory Syncytial Virus Type A Culture Fluid (RSV-A), Rhinovirus Type 1 A Culture Fluid (Rhino 1 A), *Staphylococcus epidermidis*, titered (*S. epidermidis*), Adenovirus Type 1 Culture Fluid (Adenovirus), and Enterovirus Type 68 Major Group Culture Fluid (Enterovirus) were purchased from ZeptoMetrix LLC (Buffalo, NY, USA) (Table S1, **SI**). The media sample of HIV culture fluid (10% RPMI) was supplied by ZeptoMetrix LLC (Buffalo, NY, USA, Lot# 561954). Saliva was collected from two donors using the IRB 2021–9, approved by Texas Tech's Institutional Review Board (IRB). Three HIV-positive patient saliva samples were purchased from Audubon Bioscience (Houston, TX, USA) for clinical study (Table S2, **SI**).

Experimental setup.—Three electrode system consisting of a rotating disk electrode (RDE) (Pine Research Instrumentation INC., Durham, NC, USA, Model# AFMSRCE, Serial# 042007) was used during the testing, where nickel disk insert (Pine Research Instrumentation INC., Durham, NC, USA, Part# AFED050P040NI, 5.00 mm OD × 4.00 mm thick, mirror polished) was utilized as a working electrode (WE). Platinum foil (ESPI Metals, Ashland, OR, USA, Item# Knc2752, Lot# Q20825,.005 in thickness, 3N5 purity) was welded as a ring (13 mm diameter, 7 mm height) using a rocket arm spot welder (Production Products Inc., MD, USA, Model# BSP 226 RF PX1600) for the counter electrode (CE). Then, a nickel wire (Alfa Aesar, Haverhill, MA, USA, 1 mm diameter, 99.5% metal basis, Lot# X28F031, CAS# 7440-02-0) was spot welded using a SUNKKO® 737 G Battery Spot Welder (SUNKKO, Las Vegas, NV, USA, Pulse:1, Current: 99) with platinum ring for the current collector of CE. A 5 mm skinny Hg/HgO electrode (KOSLOW Scientific Co, Englewood, NJ, USA, Part# 5088, Lot# 5576 C, 20% KOH) was used as a reference electrode (RE). Hg/HgO reference electrodes are recommended for high pH solutions.[36] Fifty-milliliter beakers were used throughout all testing, and a 3D-printed lid was put on the top of the beaker to hold the CE and RE in a specific position (Fig. S1, **SI**). A labForce portable pH meter (Thomas Scientific, Swedesboro, NJ, USA, Model# TS-PH200) was used to measure the pH of the prepared solution.

Electrochemical parameters.—Gamry Interface 5000 P Potentiostat/Galvanostat/ZRA (Gamry Instruments Inc., Warminster, PA, USA, Model# 08535) was used for all the electrochemical experiments using the 7.9.0 framework version. The potential range of cyclic voltammetry (CV) was scanned from 200 mV to 650 mV at the scan rate of 25 mVs^{-1}, and 5 s time was maintained to measure the open circuit potential (OCP). A constant oxidation potential of 600 mV vs Hg/HgO was applied in chronoamperometry (CA) for 3 s at 1 ms intervals. The frequency was changed from 20,000 Hz to 0.05 Hz at the AC voltage of 10 mV rms and 600 mV of DC voltage vs Hg/HgO during the electrochemical impedance spectroscopy (EIS) measurements. The rotation of RDE was set at 1600 revolutions per minute (RPM) for CA and EIS experiments. The geometric surface area of the nickel electrode (0.196 cm^2) was utilized to measure the current density.

Initial conditioning.—A one-time 500 cycles of CV was performed in 1 M KOH to form the stable layer of $Ni(OH)_2$/NiOOH on the nickel surface after purchasing the nickel electrode using the conditions of CV for the initial conditioning.[37] The changes in the formation of Ni^{2+}/Ni^{3+} peaks were observed with the increasing number of cycles (Fig. S2, **SI**). The oxidation and reduction peaks overlapped in the last ten cycles during initial conditioning, which justified the choice of 500 cycles to condition the nickel electrode (Fig. S3, **SI**). Also, the aging of the nickel electrode facilitated the formation of β-NiOOH, which helped to sense the HIV p24 protein/ culture fluid at applied oxidation potential. If needed, the nickel electrode was polished with two different concentrations of alumina slurries, such as 0.05 and 0.3 μm on the micro cloth using the polishing kit (Pine Research Instrumentation INC., Durham, NC, USA, Part# AKPOLISH). Then, the same initial conditioning procedure was followed to prepare the nickel electrode for the next steps.

Experimental steps for chronoamperometry.—The experiment started with three cycles of CV following the above conditions using 1 M KOH to form NiOOH electrocatalyst on the nickel surface and then performed OCP for 5 s to measure the system's stability with 0.01 M KOH and finally operated CA for 3 s under applied oxidation potential of 600 mV vs Hg/HgO to measure the current response using the unchanged solution of OCP at 1600 RPM. Kimwipes were used for the electrodes to eliminate the carryover from 1 M KOH to 0.01 M KOH. These three steps were utilized for the following baseline/sample tests. Sample tests were carried out by adding HIV p24 protein/HIV culture fluid/Influenza A NP protein/HBV Capsid protein/saliva/saliva with different pathogens in 0.01 M KOH, and the baseline was performed only with 0.01 M KOH for both OCP and CA measurements. In this method, the baseline experiment is always performed first before conducting any sample tests to measure the current difference between the respective baseline and sample. So, the sensor has a dynamic baseline that would minimize manufacturing variability when using multiple sensors. This approach was successfully demonstrated by Botte et al. during the selective detection of SARS-CoV-2 using four different sensors.[38] Finally, the nickel electrode was rinsed with 1 M KOH before performing the subsequent test to reduce the interferences from the previous test.

Conditioning the setup.—Fifteen cycles of CV were carried out at the beginning of the day (before testing), and then three different baseline vs baseline tests were performed following the above conditions. The current response of baseline vs baseline test overlapped respectively due to having similar NiOOH formation in both cases at least for 10 ms (Fig. S4, **SI**). If the nickel electrode met these conditions and showed a similar response, it moved forward for the sample test. If it failed to follow a similar current behavior, those steps were repeated until it exhibited an almost identical response during the baseline test.

Electrochemical impedance spectroscopy.—EIS was conducted after three cycles of CV to measure the resistance following the above conditions at 1600 RPM, and 1 M KOH was used in both cases. These two steps were followed for the successive baseline/sample tests. Baseline tests were performed only with 1 M KOH, and sample tests were conducted by adding different amounts of HIV culture fluid with 1 M KOH to distinguish the resistance in the presence of HIV culture fluid.

HIV p24 protein preparation.—The initial concentration of HIV p24 protein was 0.4 $\mu g\ \mu l^{-1}$. HIV p24 protein was diluted with a 1:10 dilution (10 μl in 90 μl of deionized water) to achieve a concentration of 0.04 $\mu g\ \mu l^{-1}$. Then, aliquots (5, 10, 20, 30, and 40 μl) of the diluted HIV p24 protein solution were added to solutions of 0.01 M KOH to make the final volume of 17000 μl. The volume of all solutions was always maintained at 17 ml. Also, 100 μl of HIV p24 protein buffer was added to 0.01 M KOH solution to assess buffer interference.

Influenza A NP protein and Hepatitis B Virus Capsid protein preparation.—Lyophilized Influenza A nucleoprotein (NP) and Hepatitis B virus (HBV) Capsid protein were reconstituted in sterile deionized water and buffer solution (150 mM NaCl, 50 mM Tris, pH 7.0), respectively, to a final concentration of 0.25 $\mu g\ \mu l^{-1}$. Aliquots (30 and 50 μl) of each protein solution were added in 0.01 M KOH

to a final volume of 17000 μl separately. 100 μl of the HBV capsid protein buffer (150 mM NaCl, 50 mM Tris, pH 7.0) was added to 0.01 M KOH solution to assess buffer interference.

HIV CF preparation.—HIV culture fluid from two distinct lots was utilized in this study. Lot 1 (initial titer: 4.07×10^7 $TCID_{50}$ ml^{-1}) was employed for response characterization and linearity analysis, while Lot 2 (initial titer: 5.56×10^6 $TCID_{50}$ ml^{-1}) was used for electrochemical impedance spectroscopy (EIS) and saliva-based experiments.

Preparation of HIV CF using lot 1.—The HIV culture fluid was serially diluted with deionized water, starting with a 1:100 dilution (20 μl in 1980 μl) to achieve an initial concentration of 4.07×10^5 $TCID_{50}$ ml^{-1}. Three subsequent serial dilutions yielded a final concentration of 0.407 $TCID_{50}$ ml^{-1}. Aliquots (20, 30, 40, and 50 μl) of the final dilution were added to 0.01 M KOH solutions, maintaining a total volume of 17 ml for electrochemical analysis. The 10% Roswell Park Memorial Institute (RPMI) medium control experiments were conducted using diluted and undiluted samples. The diluted RPMI followed identical dilution protocols to the HIV culture fluid, with equivalent volumes added to 0.01 M KOH solutions. Additionally, 100 μl of undiluted 10% RPMI was introduced to 0.01 M KOH to assess the medium's electrochemical response.

Preparation of HIV CF using lot 2.—HIV culture fluid was initially diluted 1:13.5 (74 μl in 926 μl deionized water) to achieve 411,440 $TCID_{50}$ ml^{-1} concentration. Six sequential 1:10 dilutions (100 μl in 900 μl deionized water) yielded a final concentration of 0.411440 $TCID_{50}$ ml^{-1}. For electrochemical impedance spectroscopy (EIS) measurements, aliquots (200 and 400 μl) of the final dilution were added to 1 M KOH solutions. For saliva-based experiments, three volumes (22, 44, and 55 μl) of the 0.411440 $TCID_{50}$ ml^{-1} HIV culture fluid were spiked into saliva samples to a final volume of 1100 μl. Subsequently, 1000 μl of each HIV-spiked saliva solution was transferred to 16 ml of 0.01 M KOH, maintaining a final volume of 17 ml across all experiments.

Saliva preparation.—Saliva specimens were collected from two donors under IRB-approved protocol 2021–9 as negative controls. Donors abstained from food consumption for a minimum of 1 h pre-collection to minimize food residue contamination. Specimens were stored at −20 °C until analysis. Aliquots were withdrawn from the middle portion of each specimen vial to minimize mucous content. Two volumes (500 and 1000 μl) of each donor's saliva were introduced into 0.01 M KOH solutions for electrochemical analysis. Measurements were performed using three independent samples for each volume and donor to determine standard deviations.

Preparation for cross-reactivity study.—For cross-reactivity analysis, each pathogen suspension (excluding HIV culture fluid) was prepared by introducing 55 μl of stock solution into 1045 μl of saliva matrix. Subsequently, 1000 μl of each pathogen-spiked saliva solution was transferred to 16 ml of 0.01 M KOH. HIV culture fluid was diluted to 0.411440 $TCID_{50}$ ml^{-1} and processed following identical protocols. All pathogen preparations were conducted independently, with three different sample measurements completed before proceeding to the other pathogen species.

Preparation for clinical study.—Clinical validation was performed using saliva specimens from three HIV-positive patients. For electrochemical analysis, 1000 μl of each patient specimen was introduced into 16 ml of 0.01 M KOH. Measurements were conducted using three discrete samples for each patient specimen to assess reproducibility and determine standard deviations.

Results and Discussion

Electrocatalyst formation and system stability.—Initially, the nickel electrode formed $Ni(OH)_2$ chemically in the presence of KOH, an alkaline medium, and it produced NiOOH as an electrocatalyst on the nickel surface at an applied potential to facilitate HIV detection after that. The formation of the electrocatalyst was stabilized by performing a cyclic voltammetry test in 1 M KOH until a sustained periodic state was reached (Fig. 2a). The third cycle of CV represented the stable cycle after cycling three times, where it produced NiOOH at 540 mV vs Hg/HgO during the oxidation and $Ni(OH)_2$ at 460 mV vs Hg/HgO during the reduction (Fig. 2a). The oxidation and reduction reaction is represented in equation (1), which shows the reversible reaction of one electron transfer between $Ni(OH)_2$ and NiOOH.[39]

$$Ni(OH)_2 + OH^- \rightleftharpoons NiOOH + H_2O + e^- \quad [1]$$

The open circuit potential (OCP) measurements demonstrated electrode stability, with negligible potential drift observed over 5 s intervals in two different 0.01 M KOH solutions, confirming that the nickel electrode had reached equilibrium under these conditions

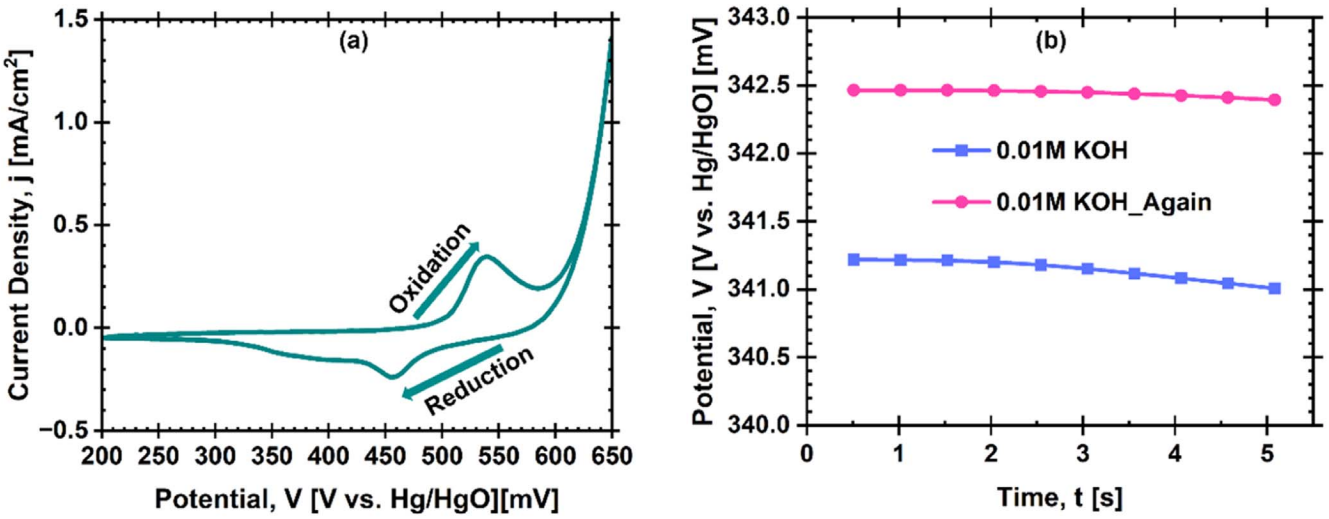

Figure 2. Formation of the electrocatalyst and displaying stability of the system. (a) A plot of the third cycle of cyclic voltammetry of nickel electrode in 1 M KOH scanned from 200 mV to 650 mV at the scan rate 25 mVs^{-1}, where the oxidation peak showed at around 540 mV and reduction peak exhibited at around 460 mV. The formation of NiOOH acted as an electrocatalyst for the detection of HIV. (b) The plot represents the open circuit potential response of two different 0.01 M KOH solutions, where the potential changed in the range of ±5 mV, which indicated the system's stability.

(Fig. 2b).[40] The established OCP values served as reference points for determining the appropriate oxidation potential range for NiOOH formation, which was subsequently investigated using chronoamperometric analysis of the sensor.[40]

Electrochemical response of HIV p24 protein and culture fluid.—The sensor was tested for HIV detection after generating an electrocatalyst on the electrode surface. HIV p24 protein was used initially for the detection as it is the only protein that can be available in the patient's body in the initial days of HIV infection.[41] A buffer solution of 0.01 M KOH was spiked with different concentrations of HIV p24 protein, ranging from 11.76 ng ml^{-1} to 94.12 ng ml^{-1}, to explore the interaction of HIV p24 protein with the sensor. A baseline experiment was performed with a buffer solution of 0.01 M KOH before experimenting with HIV p24 protein in the baseline. This experiment was conducted to compare the current response between baseline and HIV p24 protein in the baseline. The electrical current response sharply declined from the baseline in the presence of HIV p24 protein (Fig. 3a). Similar experiments comparing the HIV p24 protein buffer with the 0.01 M KOH baseline indicated that the buffer did not affect the electrochemical response of the baseline (Fig. S5a, **SI**). The observed attenuation in amperometric response can be attributed to the selective binding of HIV p24 protein to the electroactive sites on the nickel electrode surface. This interaction, occurring at the applied oxidation potential and specified time interval, inhibits the forward kinetics of the Ni^{2+}/Ni^{3+} redox transition described in equation (1), resulting in reduced chronoamperometric current signals. Similar characteristics were observed in previously reported studies.[31,42] The limit of detection (LOD) for the HIV p24 protein of this sensor was 11.76 ng ml^{-1} (Fig. S5b, **SI**).

The sensor was probed with different concentrations of HIV culture fluid (HIV CF) in 0.01 M KOH to examine the interactions of HIV CF with the sensor and to investigate whether the sensor showed a comparable response of HIV p24 protein with HIV CF response. The ranges of the HIV CF concentration were from 47.80×10^{-5} $TCID_{50}$ ml^{-1} to 119.70×10^{-5} $TCID_{50}$ ml^{-1}, and the unit conversion between $TCID_{50}$ ml^{-1} and copies ml^{-1} is that 1 $TCID_{50}$ ml^{-1} of HIV culture fluid almost equals to 10^2 to 10^5 copies ml^{-1} of HIV RNA.[43] The amperometric response to HIV CF in 0.01 M KOH exhibited lower current densities than the 10% RPMI control, closely paralleling the response pattern observed with purified HIV p24 protein (Fig. 3b). The analogous electrochemical behavior between HIV CF and purified HIV p24 protein suggests that the current attenuation in HIV CF samples primarily originated from p24 protein-electrode interactions. Furthermore, the comparable current density profiles between the HIV CF medium (10% RPMI) and 0.01 M KOH baseline confirmed that the culture medium components did not contribute to the observed current difference in HIV CF measurements (Fig. S6a, **SI**). Other studies have reported similar current reduction features with HIV.[44,45] The sensor can successfully distinguish a low concentration of 47.80×10^{-5} $TCID_{50}$ ml^{-1} HIV CF, which was the LOD of the sensor for HIV CF (Fig. S6b, **SI**). The OCP measurements revealed negligible potential deviation (±5 mV) between HIV CF and baseline conditions (Fig. S7, **SI**), indicating preservation of interfacial equilibrium at the electrode surface. Significant current suppression was observed during chronoamperometric measurements under applied oxidation potential. The mechanism of current attenuation can be attributed to competitive adsorption of HIV CF components at the electrocatalytic sites, which impedes the single-electron transfer process necessary for continuous NiOOH formation according to equation (1). This site-blocking effect effectively reduces the electrochemically active surface area for the Ni^{2+}/Ni^{3+} redox transition.

EIS measurements were conducted using two HIV CF concentrations (484×10^{-5} and 968×10^{-5} $TCID_{50}$ ml^{-1}) in 1 M KOH electrolyte, with 1 M KOH serving as a control, to quantitatively evaluate the electrode-analyte interfacial characteristics and verify the proposed surface site-blocking mechanism hypothesis (Fig. 3c). EIS analysis revealed concentration-dependent increases in charge transfer resistance (R_{ct}) for HIV CF samples, with ΔR_{ct} values of approximately 100 Ω and 250 Ω observed for 484×10^{-5} and 968×10^{-5} $TCID_{50}$ ml^{-1}, respectively, relative to the 1 M KOH baseline (Fig. 3c). This enhanced interfacial impedance correlates with decreased NiOOH formation kinetics at the applied oxidation potential. Comparative analyses with purified HIV p24 protein and control proteins (Influenza A NP protein and Hepatitis B virus capsid protein) demonstrate that the observed electrochemical response is specifically mediated by the characteristic surface-accessible amino acid residues of the HIV p24 capsid protein, rather than non-specific protein-electrode interactions (Figs. S10, S11, S12, S14, **SI**). A similar phenomenon was observed in the literature when using chitosan/Fe_3O_4 on screen-printed electrodes.[44] The charge transfer resistance of the three following 1 M KOH solutions decreased with successive experiments during the EIS (Fig. S8, **SI**). These attributes validated that the sensor showed a better conductivity at that oxidation potential in the absence of HIV cf

The sensor's electrochemical response was characterized across a concentration series of HIV CF (47.8×10^{-5}, 71.8×10^{-5}, 95.7×10^{-5}, and 119.7×10^{-5} $TCID_{50}$ ml^{-1}) to evaluate the concentration-dependent interfacial interactions (Fig. 3d). Differential current density measurements were obtained by comparing the amperometric responses between HIV CF samples and 10% RPMI control in 0.01 M KOH electrolyte, using three different samples measurements performed to establish statistical validity. The observed linear increase in differential current density with HIV CF concentration demonstrates progressive inhibition of the electrocatalytic surface, manifesting as enhanced current attenuation at higher analyte concentrations (Fig. 3d). This concentration-dependent behavior provides quantitative evidence for HIV CF-mediated suppression of the Ni^{2+}/Ni^{3+} oxidation process at the applied potential.

The 1 ms point of the current density difference of four different HIV CF concentrations was utilized to generate the linearity study of the sensor (Fig. 3e). The current density difference was almost linear with increasing the concentration of HIV CF, demonstrating a high R^2 value (almost ∼1).

Performance of saliva and HIV CF in saliva.—Human saliva is mainly constituted of water, a small portion of organic molecules, and different proteins such as glycoproteins, enzymes, and mucins.[46,47] Two different amounts of saliva such as 500 and 1000 μl, were used from two donors to explore the interactions of the sensor with the human saliva using three different samples of each, where % current difference with respect to the baseline for the 1 ms point was equated using equation (2) (Fig. 4a).

$$\%\mathit{Current\ Difference\ w.r.t\ Baseline} = \left(\frac{(\mathit{Baseline\ Current} - \mathit{Sample\ Current})}{\mathit{Baseline\ Current}} \times 100\right) \quad [2]$$

The sensor showed a lower current response in the presence of saliva. The decreased current was higher with the increasing amount of saliva, which is why the current difference was higher during 1000 μl of saliva compared to 500 μl of saliva (Fig. 4a). The probable reason for lowering electrical current density when using saliva is that saliva has different electrochemically inert molecules and organics, which can be adsorbed to the electrode surface.[48] These molecules may be responsible for reducing the electroactive surface area of the sensor. Also, saliva has a pH range of 6.2–7.6, which reduced the bulk pH of the saliva and 0.01 M KOH solution with the increasing amount of saliva.[49] So, the lowering pH affected the forward equation of (1) during the applied oxidation potential. 1000 μl of saliva was chosen to add with 16,000 μl of 0.01 M KOH for the following experiments based on the hypothesis that a higher amount of saliva will contain more HIV. Based on fourteen different sample tests using two healthy donors and their impact on the

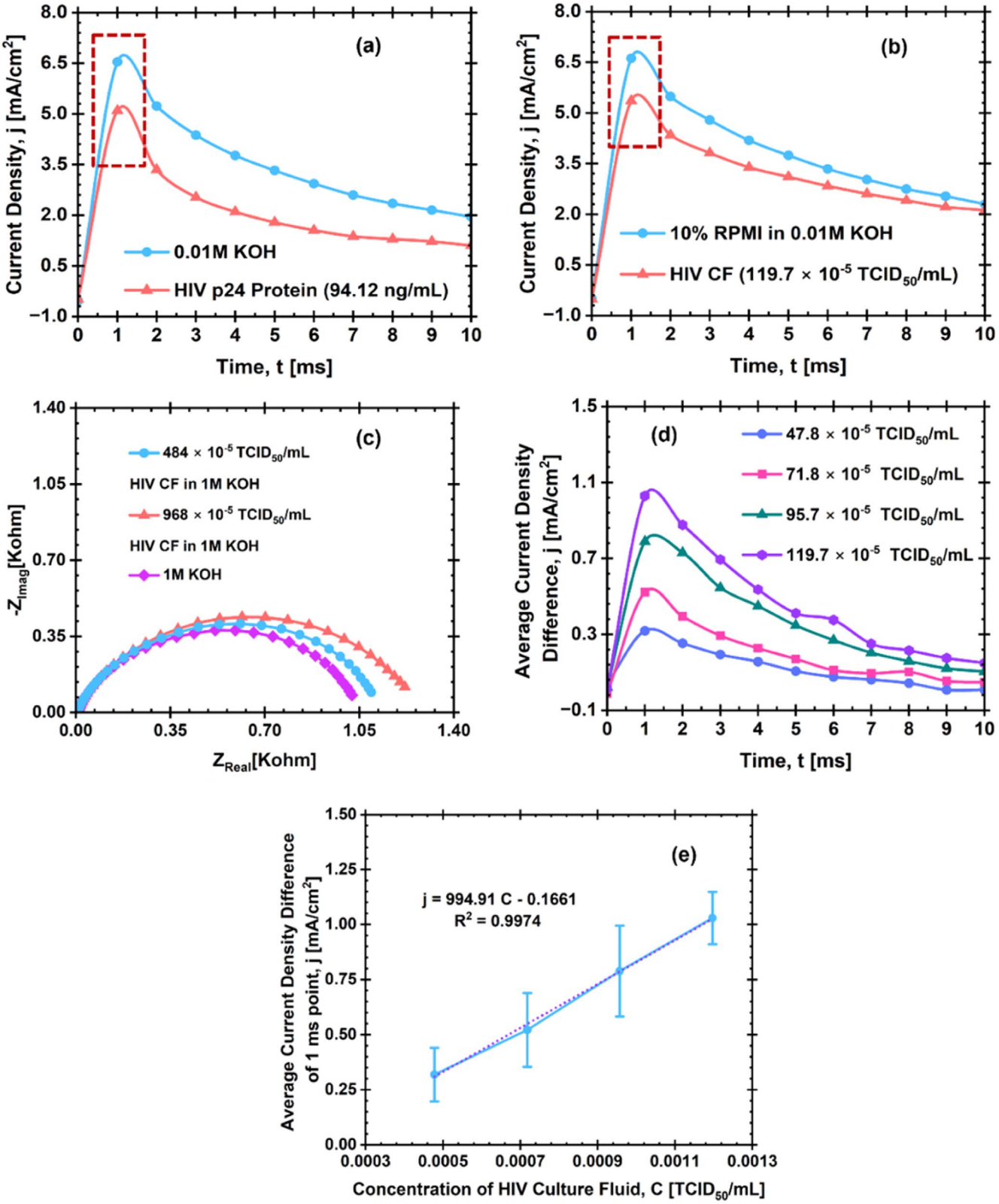

electrolyte, it was concluded that a 7.5% current difference would be the maximum difference for the saliva, capturing different variability (Fig. 4c).

Three different concentrations of HIV CF, such as 48.4×10^{-5}, 96.8×10^{-5}, and 121.0×10^{-5} $TCID_{50}$ ml^{-1}, were spiked into saliva to mimic a real scenario and investigate the sensor's capacity to distinguish HIV's response from the saliva (Fig. 4b). Three experiments were conducted for each HIV CF concentration, and equation (2) was used to calculate the % current difference with respect to the baseline for the 1 ms point. The sensor successfully differentiated the HIV response from the saliva, showing a higher than 7.5% current difference of all three concentrations, which was

Figure 3. Electrochemical performance of HIV p24 protein and HIV culture fluid. (a) Chronoamperometry plot showing the current density of baseline (0.01 M KOH) vs HIV p24 protein in 0.01 M KOH at an applied oxidation potential of 600 mV vs Hg/HgO for 10 ms, where the current response dropped in the presence of HIV p24 protein. (b) The plot represents the electrical current response of 10% RPMI in 0.01 M KOH and HIV CF in 0.01 M KOH at an applied oxidation potential of 600 mV vs Hg/HgO for 10 ms, with similar attributes exhibited by HIV CF of HIV p24 protein. These features facilitated the detection of both HIV CF and HIV p24 protein. (c) The Nyquist plot represents the EIS of 1 M KOH and HIV CF in 1 M KOH, where the frequency changed from 20 kHz to 0.05 kHz at the 10 mV rms AC voltage, 600 mV vs Hg/HgO DC potential and 1600 RPM rotation. The charge transfer resistance increased in the presence of HIV CF, which justified the decreased current response during the chronoamperometry. (d) The chronoamperometry plot represents the average current density difference between 10% RPMI in 0.01 M KOH and HIV CF in 0.01 M KOH, where four different concentrations of HIV CF were used, and three independent samples were prepared for each concentration. The average current density difference increased with the increasing concentrations of HIV CF, which implies that the higher the concentration of HIV CF, the lower the current response. (e) The average current density difference for the 1 ms point was used to develop the linear regression of the response with the concentration of HIV cf The linear fit equation is: j $(\frac{mA}{cm^2}) = 994.91$ C $(\frac{mA}{cm^2})$—0.1661 $(\frac{mA}{cm^2})$, where j is the average current density difference for the 1 ms and C is the concentration of HIV cf.

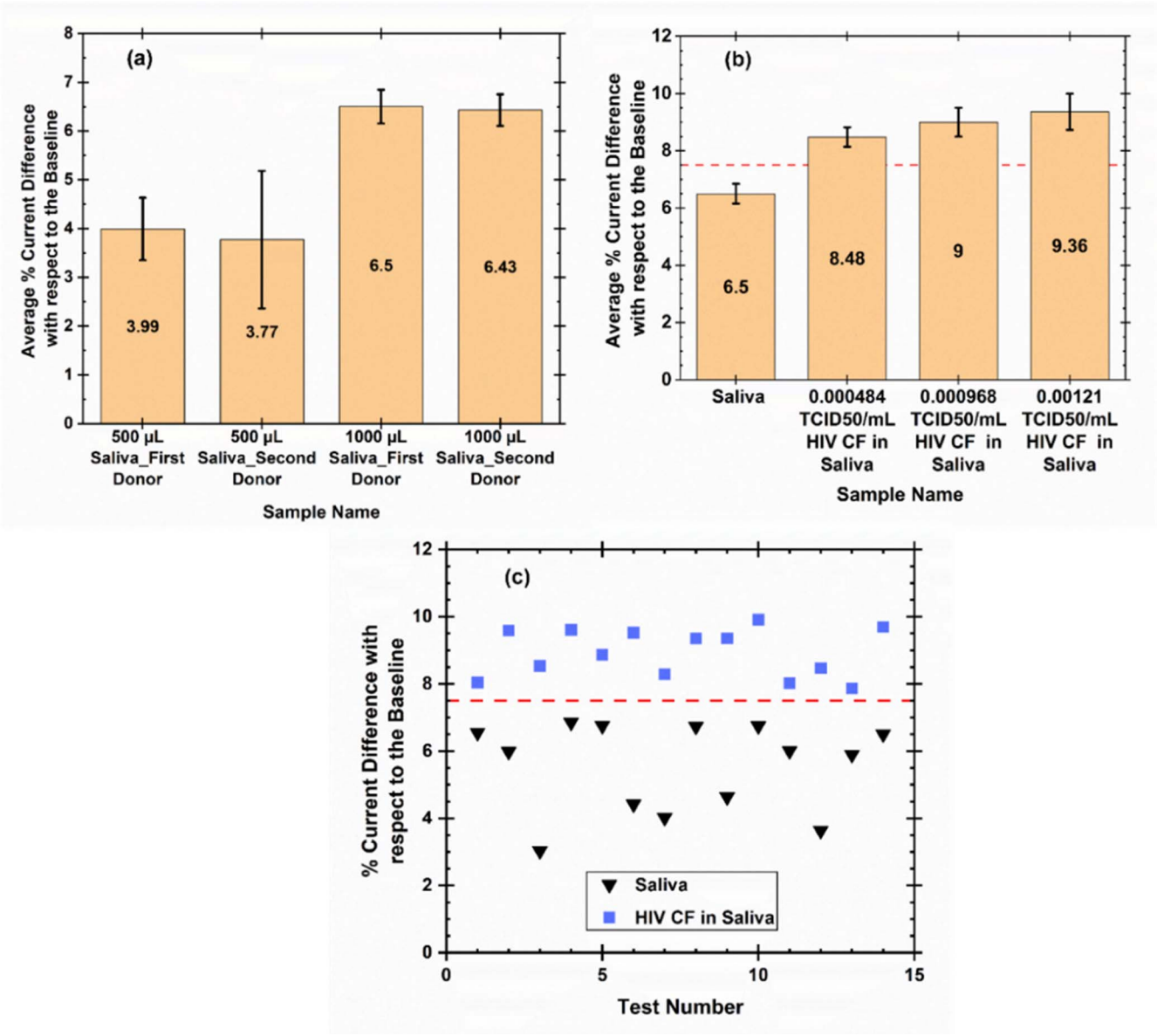

Figure 4. Saliva's electrochemical response in 0.01 M KOH and electrical current response comparison of saliva and HIV CF in saliva. (a) The bar plot shows the average % current difference with respect to the baseline of the 1 ms of two different amounts of saliva added with a specific amount of 0.01 M KOH (the final volume of the mixed solution was maintained at 17 ml) using two distinct donors over three different tests for each case. The current difference increased with the increasing amount of saliva in 0.01 M KOH, and the difference was almost the same for two different donors in both amounts of saliva. (b) The bar plot represents the average % current difference with respect to the baseline of 1 ms for saliva and three different concentrations of HIV CF in saliva, where three trials were used to measure the standard deviation. HIV CF exhibited a higher current difference compared to the saliva, which helped to detect HIV CF in saliva over saliva. (c) The scatter plot shows the average % current difference with respect to the baseline of the 1 ms for saliva and HIV CF in saliva using fourteen different tests in both cases. The final concentration of HIV CF in saliva was 48.4×10^{-5}, 96.8×10^{-5}, and 121.0×10^{-5} $TCID_{50}\,ml^{-1}$. HIV CF in saliva dominates over saliva in all these tests, where a 7.5% current difference was chosen for the maximum changes for saliva. Saliva from two distinct donors was used for the saliva testing.

the criteria chosen for HIV detection in saliva (Fig. 4b). The minimum charge of NiOOH formation required to detect HIV CF in saliva successfully was 70.85 μC (Fig. S9, **SI**). The LOD of HIV CF in the saliva is ~50 copies ml^{-1} computed using the maximum conversion factor between $TCID_{50}$ ml^{-1} and copies ml^{-1} (1 $TCID_{50}$ ml^{-1} ≈ 10^2 to 10^5 copies ml^{-1} of HIV RNA).[43] The LOD could be lower if other conversion factors were utilized. The ability of the sensor to detect 50 copies ml^{-1} of HIV CF in saliva made it eligible for cross-reactivity studies and clinical trials. The hypothesis of having a high current drop during the presence of HIV in the saliva is that HIV may lower the active site of the nickel electrode more compared to the saliva or partly slow down the diffusion of OH^- ions to the electrode, which results in the lower formation of NiOOH at the applied oxidation potential. The results of fourteen different experiments for both HIV CF in saliva and saliva are represented, where equation (2) was used to determine the % current difference with respect to the baseline for the 1 ms point in both cases (Fig. 4c). The final concentration of HIV CF in saliva was 48.4×10^{-5}, 96.8×10^{-5}, and 121.0×10^{-5} $TCID_{50}$ ml^{-1}. HIV CF in saliva showed a higher current difference compared to the saliva in all fourteen experiments (Fig. 4c). A t-test was performed to determine a statistically significant difference between saliva and HIV culture fluid in saliva sample responses (Fig. 4c). The p-value was lower than 0.0001 in the t-test, which suggests that HIV in saliva and saliva responses were statistically different (Fig. 4c). The higher number of tests validated the sensor's reliability and reproducibility with the HIV CF response in saliva.

Cross-reactivity study.—HIV-infected patients are more likely to have different opportunistic infections due to having a suppressed immune system.[50] Hepatitis B Virus (HBV), Epstein-Barr Virus (EBV), Cytomegalovirus (CMV), and Herpes Simplex Virus-1 (HSV-1) are the most common co-infections for HIV patients.[50–52] Also, Influenza A (INF-A), Influenza B (INF-B), Human Metapneumovirus (hMPV), Respiratory Syncytial Virus (RSV-A), Rhinovirus (Rhino 1 A), Staphylococcus epidermidis, Adenovirus, and Enterovirus can be found in saliva at a different concentration varying in the patients and have similar symptoms of HIV during the initial days of the infection.[53–55] So, these pathogens are crucial when there is a concern of co-infection for HIV patients. Twelve different pathogens were spiked into saliva to challenge the sensor for distinguishing HIV CF responses over those pathogens' responses (Fig. 5). The final concentration of these pathogens in saliva and their approximate range in saliva are shared to justify the final concentrations matched with the approximate range (Table S3, **SI**). The concentrations of other pathogens were high compared to the available ranges of those pathogens in the saliva (Table S3, **SI**). On the other hand, the concentration of HIV CF in saliva was almost 5 to 10 orders less compared to these pathogens in saliva as it was diluted multiple times to determine the limit of detection of HIV in saliva and made the sensor eligible for clinical trials (Table S3, **SI**). Three different samples were used for each pathogen, and equation (2) was applied to enumerate the % current difference with respect to the baseline for the 1 ms point of each pathogen.

All the other pathogens showed a less than 7.5% current difference, which is in the range of saliva response and lower than the threshold for HIV detection (7.5% current difference is the maximum difference of saliva) (Figs. 5, 4c). On the other hand, HIV was the only virus that passed the threshold (>7.5%) and showed a positive response (Fig. 5). HIV responded more to the sensor than other pathogens at the oxidation potential. Finally, the maximum variability of the responses of Gamry potentiostat is ±0.2%, which is negligible compared to the threshold of 7.5%.[56] So, the hypothesis of having these attributes of HIV is due to the inhibition of the nickel electrode surface by HIV at that applied oxidation potential. The sensor's ability to differentiate HIV's response from similar viruses/bacteria in saliva warranted the sensor's specific detection of HIV.

Clinical study.—It is crucial to verify the sensor's performance with the HIV-positive patient's saliva, where the hypothesis is that HIV-positive patients contain a high viral load in the initial days of infection if they do not start any treatment.[18] Three positive patients' saliva was utilized over three independent samples for each patient to investigate the response of the sensor to the HIV patient's saliva (Fig. 6). The % current difference with respect to the baseline for the 1 ms point of each patient's saliva sample was determined using equation (2). As these patients were at their starting period of the infection, they might have a detectable viral load in their saliva (Table S2, **SI**).

The sensor favorably detected two patients' samples showing more than 7.5% current difference with respect to the baseline out of three patients (Fig. 6). CV-27005S patient saliva sample showed a mean of almost 14% current difference over three different samples, which verified that this patient might have a higher viral load in saliva (Table S4, **SI**). Also, the day difference between the diagnosis and donation of the saliva for this patient was less than one month, which also justified the hypothesis of having a high HIV concentration in saliva in the initial period of infection (Table S2, **SI**). Although the second patient CV-27004S also fulfilled the detection standard, exhibiting an average of 8.28% current difference for three different trials, the third patient CV-27003S saliva sample did not reach a 7.5% current difference in any of their three different samples (Table S4, **SI**). The probable reason for not getting a 7.5% current difference was that the third patient's saliva did not have enough HIV concentration to detect with the sensor. The time between diagnosis and saliva donation was around 70 days for both the second and third patients, which could be the possibility that the third patient had less concentration than the second patient due to having different immune systems and distinct body responses to certain infections (Table S2, **SI**). As the concentration of HIV p24 protein or HIV RNA declines with time in the blood, those concentrations can decrease in saliva.[57] These three patients had co-morbidities of Hepatitis B(HBV) infection along with HIV (Table S2, **SI**). As our sensor successfully detected HIV (more than 7.5% current difference) over HBV (less than 7.5% current difference) in the cross-reactivity study, it justified that HIV possessed a higher current density difference for these three patients (Fig. 5). Also, the three samples of the second patient were tested on three different days to analyze the stability of the sensor. The sensor successfully exhibited more than 7.5% on each day of testing, exemplifying high stability (Table S4, **SI**). Testing with more HIV-positive patients' saliva will benefit the sensor to commercialize it as a non-invasive sensor.

Hypothesized mechanism.—HIV p24 protein and HIV CF showed similar current reduction characteristics with the sensor compared to the baseline (0.01 M KOH), which means the whole virus cell may break down to proteins at high pH in the presence of HIV CF exhibiting corresponding response of HIV p24 protein.[58] It is hypothesized that these proteins may inhibit the active surface area of the nickel electrode at the applied oxidation potential, resulting in decreased current density. At high pH, proteins undergo denaturation due to alterations in charge distribution, exposing their constituent amino acid residues.[59] The electrochemically active amino acids present in HIV p24 protein, particularly methionine and tryptophan (Fig. S10, **SI**), could contribute to the reduced current response at the applied potential.[60–62] The bulky side chains of these amino acids—specifically the indole rings of tryptophan and sulfur-containing groups of methionine (Fig. S10, **SI**)—might adsorb to the $Ni(OH)_2$ surface, potentially occupying a significant portion of the electrochemically active sites (Figs. 7a, 7b). It is proposed that when these amino acid residues interact with the electrode surface in the presence of HIV p24 protein or HIV CF, they may lead to a localized depletion of OH^- ions at the electrode/electrolyte interface (Figs. 7a, 7b). This proposed mechanism of hydroxide ion depletion could account for the observed decrease in current compared to measurements taken in their absence.

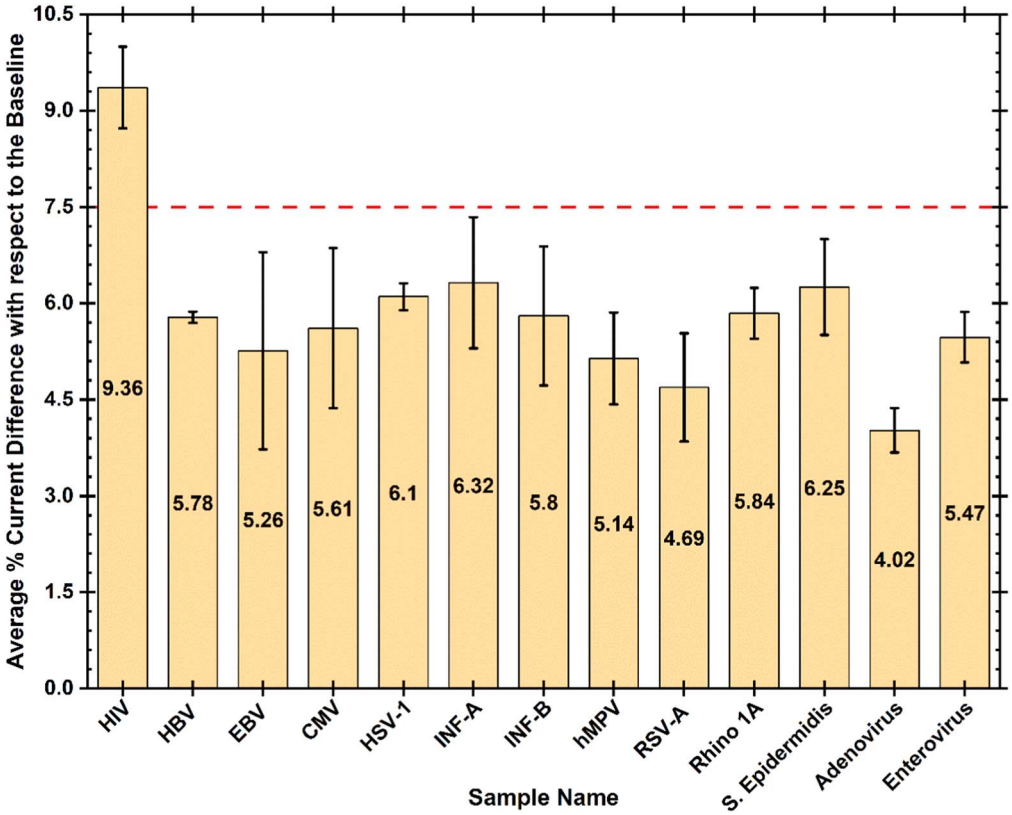

Figure 5. Cross-reactivity study of twelve different pathogens in saliva to compare with the response of HIV culture fluid. The plot represents the cross-reactivity study of twelve different pathogens in saliva to check the sensor's cross-reactivity over similar pathogens of HIV. HIV showed a higher than the maximum current response of saliva (7.5%), whereas all the other pathogens exhibited lower than the maximum current response. HBV, EBV, CMV, and HSV-1 are the most common co-infections for HIV-infected patients, and other pathogens can be available in saliva.

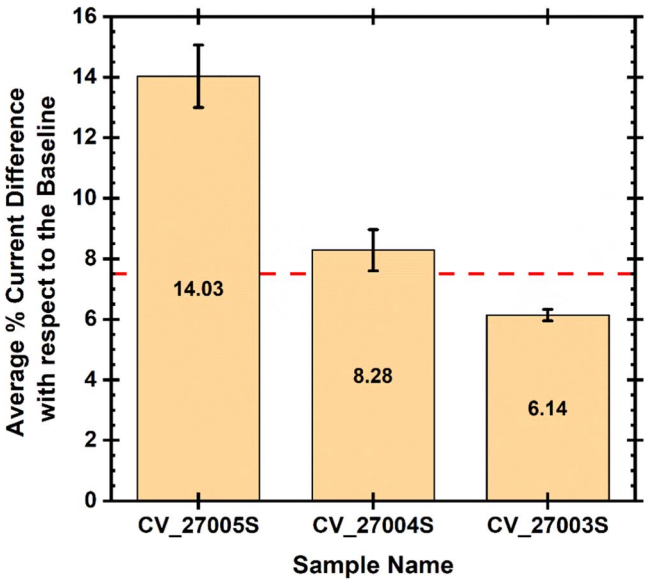

Figure 6. A clinical study was performed with three HIV-infected person's saliva. The plot shows the clinical study of three HIV-infected patients' saliva, where the sensor successfully detected HIV in two patients' saliva out of three patients. Three different samples were conducted for each patient, and a 7.5% current difference concerning the baseline was chosen as a cutoff for the detection.

Two different proteins such as Influenza A NP protein and HBV Capsid protein were compared with the performance of the HIV p24 protein to provide a better understanding of the mechanism. These proteins introduce different properties and functional groups with respect to the HIV p24 protein, indicating the selectivity of the electrochemical sensor to the HIV p24 protein within the applied potential and conditions of the experiment (pH, Time Frame) (Fig. S10, **SI**).[63,64] Influenza A NP protein is one of the virus's proteins found in the saliva, which is why it was introduced to explore the protein's response with the sensor.[65] HBV Capsid protein was utilized to compare the analogous protein of HIV Capsid protein (HIV p24 Protein). Influenza A NP protein increased the current response from the baseline, which is the opposite response of HIV p24 protein (Fig. S11, **SI**). Influenza A NP protein has a tyrosine amino acid that contains OH^- ions in the side chain (Fig. S10, **SI**).[63] The excess OH^- ions may facilitate increasing the current response at the applied potential during the presence of Influenza A NP protein (Fig. 7c). On the other hand, the concentrated HBV Capsid protein's current response overlapped with the baseline current response, as it contains different amino acids, which were not reactive with the $Ni(OH)_2$ surface at these conditions (potential, pH, Time Frame) (Figs. 7d, S10, S12, **SI**).[64] Also, the buffer of HBV Capsid protein did not cause any interference with the baseline's current response (Fig. S13, **SI**). Finally, different proteins exhibited different responses at the same potential, pH, and time scale that eased the specific detection of HIV p24 protein with the sensor (Fig. S14, **SI**).

Saliva also possessed a lower current response due the presence of inert molecules and a lower pH range.[48] However, HIV CF exhibited a higher current reduction than saliva, which suggests stronger interactions of the HIV CF with the electrode than saliva at the applied potential. These hypotheses could be further investigated using in situ spectroscopy characterization techniques.

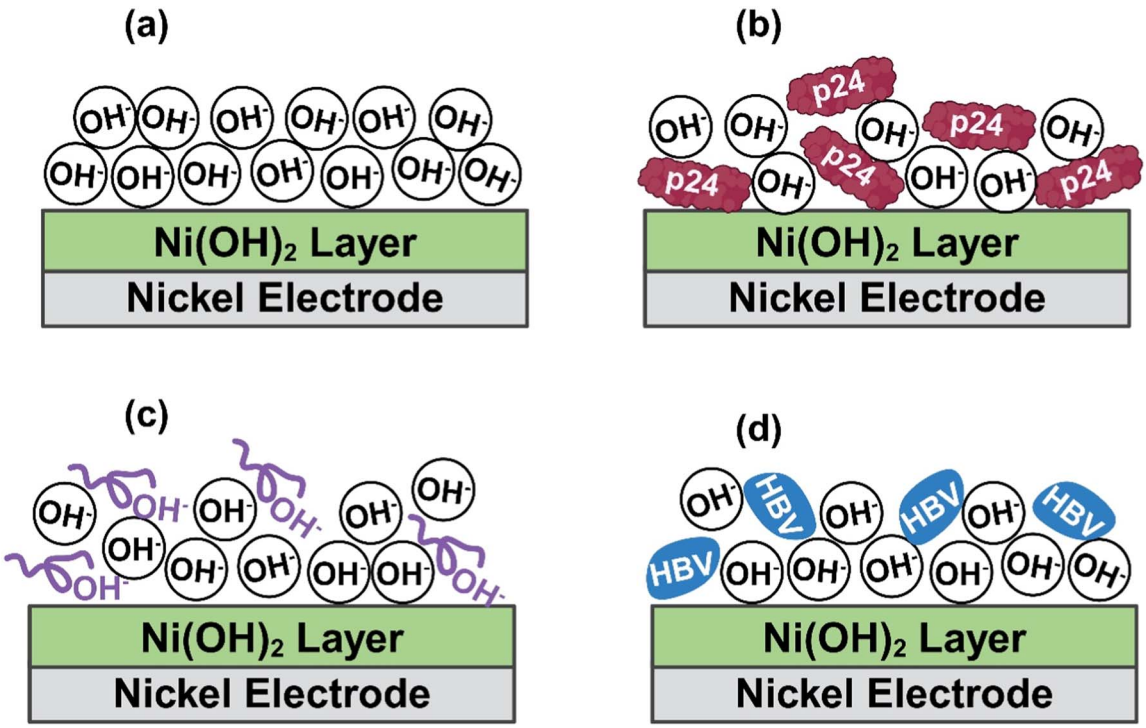

Figure 7. Schematic representation of electrode/electrolyte interface. (a) The schematic shows the electrode/electrolyte interface without proteins, where hydroxyl ions diffused to the nickel hydroxide layers to form nickel oxyhydroxide at the applied oxidation potential. (b) The presence of HIV p24 protein reduced the surface area of nickel hydroxide as HIV p24 protein binds to the surface. This binding lowers the availability of hydroxyl ions to interact with nickel hydroxide to form nickel oxyhydroxide at the applied oxidation potential, which reduces the current response. (c) The presence of Influenza A NP protein increased the availability of hydroxyl ions to the nickel hydroxide surface as tyrosine has hydroxyl ions in its side chain. The excess hydroxyl ions may facilitate increasing the current response at the oxidation potential during the presence of Influenza A NP protein. d) HBV Capsid protein was not reactive with the nickel hydroxide surface at these conditions (potential, pH, Time Frame), so the protein did not alter the current response from the baseline.[66].

Conclusions

In summary, we developed an electrochemical biosensor to detect HIV in saliva by forming the NiOOH electrocatalyst. The facile and rapid detection technique of this sensor will lower the concern of patients as the whole detection procedure takes around 15 min. More importantly, one of the significant advantages of this sensor is that the detection method did not require immobilization, which made it label-free, and the enhanced rotation minimized the mass-transfer limitations. Also, the sensor's better LOD and detectable response of HIV compared with twelve different pathogens in saliva made it suitable for resource-limited settings. Future developments of this platform could incorporate artificial intelligence and machine learning models to enable automated, specific detection of multiple pathogens based on their distinct current responses. Additional work will focus on miniaturizing the sensor for point-of-care applications, followed by clinical trials with a larger cohort to validate its diagnostic utility. Implementation of in situ Raman spectroscopy would be beneficial to elucidate the detection mechanism and investigate the specific interactions between the NiOOH catalyst and HIV virus/p24 protein.

Acknowledgments

The authors would like to thank the Chemical and Electrochemical Technology and Innovation Laboratory (CETI-Lab), Institute for Sustainability and Circular Economy, the Whitacre Endowed Chair in Chemical Engineering, and the Whitacre Endowed Chair in Sustainable Energy, Texas Tech University, for providing the facilities and funds to conduct the research for this study. Claude.ai was used to review grammar. Figures 1, 7, and the graphical abstract were created using BioRender with a license granted to Botte.[35,66,67]

Declaration of Competing Interest

Authors Gerardine G. Botte and Ashwin Ramanujam are co-inventors of the rapid viral diagnostic sensor, US11060995B1, 2021. Gerardine G. Botte has ownership of EviroTech LLC (a non-publicly traded entity) that has acquired a license from Texas Tech University to commercialize the rapid viral diagnostic sensor.

Supplementary Information

Figures S1 to S14 in supplementary information present data related to the design of the sensor, activation, calibration, impedance spectroscopy analysis, charge calculation of NiOOH, different protein's amino acid structure, protein's electrical current response, and protein interference study. Tables S1 to S4 detail the specifications of the independent pathogens used in this study, HIV patient data, the concentration of pathogens in saliva, and clinical study results.

ORCID

Dipu Saha https://orcid.org/0000-0001-7089-7878
Ashwin Ramanujam https://orcid.org/0000-0002-2155-0437
Gerardine G. Botte https://orcid.org/0000-0002-5678-6669

References

1. UNAIDS, (2024), https://unaids.org/en/resources/fact-sheet.
2. KFF, (2024), https://kff.org/hivaids/fact-sheet/hiv-testing-in-the-united-states/.
3. L. Frescura et al., *PLoS One*, **17**, e0272405 (2022).
4. R. Boadu, G. Darko, P. Nortey, P. Akweongo, and B. Sarfo, *AIDS Res Ther*, **13**, 9 (2016).
5. J. K. Cornett and T. J. Kirn, *Clinical Infectious Diseases*, **57**, 712 (2013).
6. C. Tsai et al., *Proc. Natl Acad. Sci.*, **115**, 1250 (2018).
7. B. M. Branson, *JAIDS Journal of Acquired Immune Deficiency Syndromes*, **55**, S102 (2010).
8. T. S. Alexander, *Clinical and Vaccine Immunology*, **23**, 249 (2016).

9. N. P. Pai, A. Karellis, J. Kim, and T. Peter, *Lancet HIV*, **7**, e574 (2020).
10. C. D. Pilcher et al., *PLoS One*, **8**, e80629 (2013).
11. L. Farzin, M. Shamsipur, L. Samandari, and S. Sheibani, *Talanta*, **206**, 120201 (2020).
12. S. Masciotra et al., *Journal of Clinical Virology*, **58**, e54 (2013).
13. CDC (2023), https://cdc.gov/hiv/partners/testing/laboratorytests.html.
14. S. Campuzano, P. Yánez-Sedeño, and J. M. Pingarrón, *TrAC, Trends Anal. Chem.*, **86**, 14 (2017).
15. K. S. R. Raju, I. Taneja, S. P. Singh, and Wahajuddin, *Biomed. Chromatogr.*, **27**, 1354 (2013).
16. J. K. M. Aps and L. C. Martens, *Forensic Sci. Int.*, **150**, 119 (2005).
17. G. Gaube et al., *Sci Rep.*, **10**, 2409 (2020).
18. R. M. Selik and L. Linley, *JMIR Public Health Surveill*, **4**, e10770 (2018).
19. R. Kantor et al., *PLoS One*, **9**, e93537 (2014).
20. R. Ikeno et al., *Journal of International Medical Research*, **46**, 996 (2018).
21. M. Balamane et al., *Open Virol J*, **4**, 88 (2010).
22. D. C. Shugars, G. D. Slade, L. L. Patton, and S. A. Fiscus, *Oral Surgery, Oral Medicine, Oral Pathology, Oral Radiology, and Endodontology*, **89**, 432 (2000).
23. A. Valizadeh, N. Sohrabi, and F. Badrzadeh, *Artif Cells Nanomed Biotechnol*, **45**, 1467 (2017).
24. D. Ivnitski, I. Abdel-Hamid, P. Atanasov, and E. Wilkins, *Biosens. Bioelectron.*, **14**, 599 (1999).
25. H. O. Kaya, A. E. Cetin, M. Azimzadeh, and S. N. Topkaya, *J. Electroanal. Chem.*, **882**, 114989 (2021).
26. M. Z. H. Khan, M. R. Hasan, S. I. Hossain, M. S. Ahommed, and M. Daizy, *Biosens. Bioelectron.*, **166**, 112431 (2020).
27. A. Ramanujam, S. Almodovar, and G. G. Botte, *Processes*, **9**, 1236 (2021).
28. G. G. Botte and A. Ramanujam, *US Patent*, 11060995 (2021).
29. A. Ramanujam and G. G. Botte, *Chemical Engineering Journal Advances*, **18**, 100611 (2024).
30. J. Zhang, X. Wu, W. Yang, J. Chen, and F. Fu, *Chem. Commun.*, **49**, 996 (2013).
31. Y. Ma, X-L. Shen, Q. Zeng, H-S. Wang, and L-S. Wang, *Talanta*, **164**, 121 (2017).
32. Y. Liang et al., *Chemistry—A European Journal*, **17**, 5989 (2011).
33. F. Franceschini and I. Taurino, *Physics in Medicine*, **14**, 100054 (2022).
34. S. Guo et al., *Anal. Chim. Acta*, **1109**, 130 (2020).
35. G. G. Botte, (2024), https://BioRender.com/i01q907.
36. S. Anantharaj et al., *J Mater Chem A Mater*, **11**, 17699 (2023).
37. A. K. Taylor, A. L. Pauls, M. T. Y. Paul, and B. D. Gates, *ACS Appl. Energy Mater.*, **2**, 3166 (2019).
38. O. Gecgel, A. Ramanujam, and G. G. Botte, *Viruses*, **14**, 1930 (2022).
39. V. Vedharathinam and G. G. Botte, *Electrochim. Acta*, **108**, 660 (2013).
40. A. Peroff, (2023), https://pineresearch.com/shop/kb/software/methods-and-techniques/basic-methods/open-circuit-potential-ocp/.
41. E. R. Gray et al., *Aids*, **32**, 2089 (2018).
42. J. L. Gogola et al., *Anal. Chim. Acta*, **1166**, 338548 (2021).
43. S. Iwami et al., *Retrovirology*, **9**, 18 (2012).
44. L. D. Tran et al., *Mater. Sci. Eng. C*, **31**, 477 (2011).
45. A. C. R. Moço et al., *J. Pharm. Biomed. Anal.*, **242**, 116025 (2024).
46. K. Ngamchuea, K. Chaisiwamongkhol, C. Batchelor-McAuley, and R. G. Compton, *Analyst*, **143**, 81 (2018).
47. S. P. Humphrey and R. T. Williamson, *J Prosthet Dent*, **85**, 162 (2001).
48. K. Ngamchuea, C. Batchelor-McAuley, and R. G. Compton, *Sens Actuators B Chem*, **262**, 404 (2018).
49. S. Baliga, S. Muglikar, and R. Kale, *J Indian Soc Periodontol*, **17**, 461 (2013).
50. A. A. J. Vaillant and R. Naik, *StatPearls [Internet]* (StatPearls Publishing) (2023), https://ncbi.nlm.nih.gov/books/NBK539787/.
51. M. A. Farisyi and I. Sufiawati, *Oral Dis*, **26**, 158 (2020).
52. E. Griffin, E. Krantz, S. Selke, M. Huang, and A. Wald, *J Med Virol*, **80**, 1153 (2008).
53. P. L. A. M. Corstjens, W. R. Abrams, and D. Malamud, *Periodontol 2000*, **70**, 93 (2016).
54. J. L. Robinson, B. E. Lee, S. Kothapalli, W. R. Craig, and J. D. Fox, *Clinical Infectious Diseases*, **46**, e61 (2008).
55. Y. Ohara-Nemoto, H. Haraga, S. Kimura, and T. K. Nemoto, *J. Med. Microbiol.*, **57**, 95 (2008).
56. Gamry, https://gamry.com/potentiostats/interface/interface-5000p/.
57. C. B. Hurt, J. A. E. Nelson, L. B. Hightow-Weidman, and W. C. Miller, *Sex Transm Dis*, **44**, 739 (2017).
58. R. Asor et al., *Soft Matter*, **16**, 2803 (2020).
59. K. Hadinoto, J. K-U. Ling, S. Pu, and T-T. Tran, *Int. J. Mol. Sci.*, **25**, 6369 (2024).
60. K. Moulaee and G. Neri, *Biosensors (Basel)*, **11**, 502 (2021).
61. A. Saito and M. Yamashita, *Retrovirology*, **18**, 32 (2021).
62. T. Kobayakawa et al., *Biomolecules*, **11**, 208 (2021).
63. C-L. Liu et al., *Sci Rep.*, **6**, 21662 (2016).
64. C. Shih, S-Y. Wu, S-F. Chou, and T-T. T. Yuan, *Cells*, **10**, 43 (2020).
65. A. Sueki et al., *Clin. Chim. Acta*, **453**, 71 (2016).
66. G. G. Botte, (2024), https://BioRender.com/l91k452.
67. G. G. Botte, (2024), https://BioRender.com/m96t576.